

A Study on Smoke Behavior in a Compartment with Sprinkler System Activation -Simple Predictive Method on Mass Flow Rates Based on Experimental Study-

Mitsuru Ota¹, Yuta Kuwana¹, Yoshifumi Ohmiya¹, Ken Matsuyama² and Jun-ichi Yamaguchi³

¹ Department of Architecture, Tokyo University of Science, Japan

² Center for Fire Science and Technology, Tokyo University of Science, Japan

³ Technical Research Institute, Obayashi Corporation, Japan

ABSTRACT

Sprinklers generate a flow of downward moving gases from smoke in the upper layer of a two-layer zone within a compartment. It is necessary to determine quantitatively the flow of downward-moving gases and fire plume in order to calculate smoke behavior in a compartment with sprinkler activation. As a first, this study proposes a measurement technique of mass flow rate based on the gas analysis method since it is difficult to understand through conventional methods. Experiments were conducted on a full scale and the following results were obtained: 1) the mass flow rate of the fire plume grows with sprinkler activation and a flow of downward-moving gases grows as the heat release rate decreases and the amount of sprinkler supplied water increases. 2) A relation between the ratios of the mass flow rate penetrated to lower layer by water droplets to the mass flow rate of watering supply from SP, and of the upper (smoke) layer and the lower layer. As a result, the mass flow rate penetrated to lower layer can be computed when the mass flow rate of watering supply from SP and temperature at the smoke and lower layers are known.

KEYWORDS: Smoke, Sprinkler System, Two-Layer Zone Model, Mass Flow Rate, Gas Analysis

NOMENCLATURE LISTING

<p><i>B</i> opening width [m] <i>H</i> opening height [m] <i>M</i> molecular weight [-] <i>m</i> mass flow rate [kg/s] <i>m_f</i> burning rate [kg/s] <i>v_n</i> velocity of measurement at n [m/s] <i>X</i> volume fraction [-] <i>Y</i> mass fraction [-] Greek <i>α</i> coefficient at opening (=0.7) [-] <i>ρ</i> density [kg/m³]</p>	<p>subscripts <i>a</i> lower layer or inflow <i>D</i> outflow (jet flow) <i>E</i> downward airflow <i>e</i> entrainment air <i>f</i> fire source <i>L</i> chemical species <i>P</i> fire plume <i>S</i> smoke layer <i>∞</i> outside air</p>
--	---

1 INTRODUCTION

Sprinkler (SP) systems are one of the most important fire safety methods for controlling building fires. The Fire Services Law in Japan requires an SP System to be installed depending on the use of the building and the size. The purpose of the installation is to extinguish or to retain a fire in an early stage. For that reason, the effect of the SP system is not generally considered in the actual practice of fire safety design under the Building Standards Law in Japan, which focuses on the spread of fire. However, SP systems clearly contribute not only to retain a fire in the early stage, but also indirectly to improve evacuation safety and fire resistance. Therefore, if the effects of the SP system were to be reflected in the fire safety design, it would be possible to evaluate fire safety appropriately and also to allow more flexibility in the building design.

However, in order to appropriately evaluate the effects of the SP system on fire safety design, it is first necessary to determine how to verify the safety when the SP system is active and the range of allowable damage when the SP system is inactive. The latter case would depend on the grade of fire resistance on the walls in the compartment. Therefore, this study applied the former case in which the SP system is active to verify the safety aspects and, in particular, investigate the smoke behavior in a compartment for evacuation safety.

The evaluation method employed in the current evacuation safety design is based on a comparison between the evacuation time needed and the time when the fire-generated smoke drops to a given height which disables the evacuation [1]. This evaluation method is based on the premise that two layers are stratified in the space of, for example, a fire compartment and/or an evacuation route. One of these layers consists of smoke containing toxic substances (the upper layer), and the other is uncontaminated air (the lower layer). However, if an SP system is activated when the air is stratified into two layers, a downward jet (hereinafter, downward airflow) is generated due to water droplets from the high-pressure water injection and it transfers smoke from the upper layer to lower layer [2]. This may conflict with the premise that the lower layer is the safe area in evacuation safety design. As for the predictive model of smoke movement, the fire plume model by Zukoski et al[3]. is mainly used in actual design practice, but this model is based on an experiment performed under a calm environment. In contrast, the environment with the activated SP system is not always calm and it is possible that the increased entrainment by the fire plume could cause the descending of smoke to accelerate.

Therefore, the ultimate goal of this study is to develop a predictive model of smoke behavior when an SP system is activated, which is based on the concept of two-layer zones. For the first step, this study focused on introducing measurement methods for the important elements of the predictive mode and mass flow rates, which pass through not only each layer but also the boundary in between the inner and outer fire compartment, and studied the relation between the amount of sprinkler water applied and the mass flow rate at each measurement point.

2 PROPERTIES OF A COMPARTMENT FIRE AND A SMOKE TRANSPORT MODEL

Based on the concept of the two-layer zone model, the method to measure various types of flow rate in this study was used with the following assumptions:

- 1) There is two-layer stratification (upper and lower layers) within the compartment during SP system activation.
- 2) Due to the complexity of active layers, quantitative values for parameters such as temperature and chemical species concentration are uniform.
- 3) Transfer of mass through the boundary surface of each layer occurs only by the fire plume, downward airflow and in/outflow at the opening due to thermal buoyancy.

Figure 1 is a conceptual diagram of smoke behavior in the compartment during SP system activation. The fire source and the water application are intentionally separated in order to explain the influence of droplets of water on smoke behavior. It is also assumed that the compartment is in stationary state.

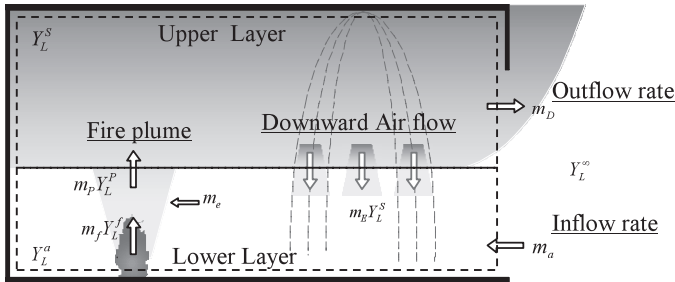


Figure 1 Conceptual diagram of the compartment

2.1 Conservation of mass

The mass flow rate [kg/s] of fire plume is calculated as follows, by using the mass burning rate of fire source m_f and the mass flow rate of entrainment air m_e :

$$m_p = m_f + m_e \quad (1)$$

The mass outflow rate m_D is calculated with the air content entrained into the lower layer, m_E (hereinafter, downward mass airflow rate), and the fire plume mass flow rate, m_p :

$$m_D = m_p + m_E \quad (2)$$

Then, the mass flow rate of entrainment air m_e is calculated by the mass inflow air into the compartment, m_a (hereinafter, inflow rate) and downward the mass airflow rate m_E

$$m_e = m_a + m_E \quad (3)$$

Mass conservation for the control volume of the entire compartment is given by the following equation, which is the sum of *Equation 1* to *Equation 3* :

$$m_D = m_f + m_a \quad (4)$$

2.2 Conservation of chemical species

By placing Y_L^p as the mass fraction of the chemical species L for the height that the fire plume penetrates into the upper layer, as the yield of the chemical species L that is generated by the combustion of the fire source and Y_L^f as the mass fraction of the chemical species L that is of the lower layer, the mass flow rate of chemical species L , which penetrates into the upper layer with the fire plume, is given the following equation by *Equation 1* :

$$Y_L^p m_p = Y_L^f m_f + Y_L^a m_a \quad (5)$$

For the chemical species conservation for the upper layer, the following equation is given by *Equation 2* :

$$Y_L^s m_D = Y_L^p m_p - Y_L^s m_E \quad (6)$$

Similarly, for obtain the chemical species conservation of the lower layer, the following equation is given by *Equation 3*

$$Y_L^a m_a = Y_L^\infty m_a + Y_L^s m_E \quad (7)$$

The chemical species conservation for the entire compartment is given by the following equation, which is the sum of *Equation 5* to *Equation 7* :

$$Y_L^s m_D = Y_L^f m_f + Y_L^\infty m_a \quad (8)$$

3 MEASUREMENT METHOD FOR MASS FLOW RATE BASED ON GAS ANALYSIS

The mass flow rates at the opening, m_D and m_a , can be calculated by using the temperature of the compartment [5] and the flow velocity of the openings. However, it is impossible to use these two parameters to measure the mass flow rates of the fire plume, m_p , and the downward airflow, m_E . On the other hand, as a method to measure the fire plume flow rate m_p , Zukoski et al. proposed a method to analyze the gas concentration of the smoke captured by installing a hood directly above the fire source [4]. Also, Yamaguchi has measured the inflow rate and flow rate of a jet plume at the opening using a similar method [7].

In this study, a method that measures various flow rates with a gas analyzer was employed to measure m_D , m_a , m_p and m_E . These are important parameters in determining the smoke behavior in a compartment during SP system activation.

3.1 Equations for each flow rate

(1) Mass flow rate through the opening; m_D

The outflow rate m_D is given by the following equation by eliminating the inflow rate using *Equations. 4 to 8* :

$$m_D = \left(\frac{Y_L^f - Y_L^\infty}{Y_L^S - Y_L^\infty} \right) m_f \quad (9)$$

(2) Mass flow rate of openings; m_a

The inflow rate m_a is given by substituting *Equation 9* in *Equation 4* :

$$m_a = \left(\frac{Y_L^f - Y_L^S}{Y_L^S - Y_L^\infty} \right) m_f \quad (10)$$

(3) Mass flow rate of downward airflow; m_E

The downward airflow m_E is given by eliminating the m_e from *Equation 3* and *Equation 7* and substituting *Equation 10* :

$$m_E = \left(\frac{Y_L^a - Y_L^\infty}{Y_L^S - Y_L^\infty} \right) \left(\frac{Y_L^f - Y_L^S}{Y_L^S - Y_L^\infty} \right) m_f \quad (11)$$

When the watering system is inactive, the m_E becomes 0 according to *Equation 11* if the chemical species at the lower layer and in the air are the same ($Y_L^a = Y_L^\infty$).

(4) Mass flow rate of fire plume, m_p

The mass flow rate of fire plume m_p is given by substituting *Equations 9* and *11* in *Equation 2* :

$$m_p = \left\{ \left(\frac{Y_L^f - Y_L^\infty}{Y_L^S - Y_L^\infty} \right) + \left(\frac{Y_L^a - Y_L^\infty}{Y_L^S - Y_L^\infty} \right) \left(\frac{Y_L^f - Y_L^S}{Y_L^S - Y_L^\infty} \right) \right\} m_f \quad (12)$$

3.2 Mass fraction, Y_L

In order to obtain each mass flow rates from *Equations 9 to 12*, it is necessary to determine the mass fraction of chemical species L . However, what is obtained from the gas analysis is volume fraction, not mass fraction. Thus, the following describes how to convert the volume fraction obtained by gas analysis into the mass fraction [7].

(1) Volume fraction X_L and mass fraction Y_L of the obtained gas

Assuming that fuel burns completely and O_2 , CO_2 , N_2 and H_2O are the only contents of air, the following equation is given for the volume fraction of gas obtained at any position:

$$X_{O_2} + X_{CO_2} + X_{N_2} + X_{H_2O} = 1 \quad (13)$$

On the other hand, the following equation is given for the relation between the volume fraction X_L and the mass fraction Y_L for chemical species L :

$$Y_L = \frac{M_L X_L}{M_{O_2} X_{O_2} + M_{CO_2} X_{CO_2} + M_{N_2} X_{N_2} + M_{H_2O} X_{H_2O}} \quad (14)$$

(2) Mass fraction Y_L of chemical species L with methanol

Chemical equation for the complete combustion for methanol as a fuel is as follows:



A case of CO_2 as a tracer

While 1.5 mol of O_2 is consumed, 1 mol of CO_2 is generated. Therefore, the volume fraction of oxygen X_{O_2} in the obtained gas is given by Equation 16. Similarly, when 1mol of CO_2 is generated, 2 mol of H_2O is generated such that the volume fraction of water vapor, X_{H_2O} , is given by Equation 17

$$X_{O_2} - X_{O_2}^\infty = -\frac{3}{2}(X_{CO_2} - X_{CO_2}^\infty) \quad (16)$$

$$X_{H_2O} - X_{H_2O}^\infty = 2(X_{CO_2} - X_{CO_2}^\infty) \quad (17)$$

Here, the volume fraction of water vapor in the outside air is given by calculating the volume of absolute humidity from relative humidity. As a note, since water was not applied to the fire source directly in the intended model of this study, the water vapor generation caused by water droplets from the SP system was ignored. Nitrogen does not contribute to the chemical reaction, therefore, the volume fraction of nitrogen, X_{N_2} , is given by the following equation by substituting Equations 16 and 17 in Equation 13 :

$$X_{N_2} = 1 - X_{O_2}^\infty + X_{H_2O}^\infty - \frac{3}{2}X_{CO_2}^\infty + \frac{1}{2}X_{CO_2}^\infty \quad (18)$$

From above, the mass fraction of CO_2 , in the obtained gas, Y_{CO_2} , is given by substituting Equation 16 in Equation 18 and each molecular mass of O_2 , CO_2 , N_2 and H_2O in Equation 14 :

$$Y_{CO_2} = \frac{22X_{CO_2}}{2X_{O_2}^\infty - 5X_{CO_2}^\infty + 13X_{CO_2}^\infty + 23X_{H_2O}^\infty + 14} \quad (19)$$

Also, the mass fraction of CO_2 in fresh air is given by substituting mass fraction of CO_2 in fresh air in Equation 19 :

$$Y_{CO_2}^\infty = \frac{11X_{CO_2}^\infty}{7 + X_{O_2}^\infty + 4X_{CO_2}^\infty + 23X_{H_2O}^\infty} \quad (20)$$

(3) The yield Y_L^f of Chemical species L at the fire source combustion

According to Equation 15 where methanol is used as fuel, when the reaction of 1 mol (32 g) of methanol consumes 3/2 mol (48 g) of O_2 and generates 1mol (44 g) of CO_2 , the generation rates of CO_2 and O_2 are as follows respectively:

$$Y_{CO_2}^f = \frac{44}{32} \quad (21)$$

$$Y_{O_2}^f = -\frac{48}{32} \quad (22)$$

4 OULINE OF EXPERIMENT

4.1 *Experimental apparatus*

Figures 2 and 3 are respectively the floor plan and cross-section of the fire compartment used in this experiment. The inside dimension of this compartment was $W6500 \times D6500 \times H2700$ [mm]. The floor surface was covered by an expanded-metal screen and plywood was placed on top of the screen. One opening ($W900 \times H2100$ [mm]) was created on a wall of the compartment. In order to improve the measurement accuracy of the mass flow rate of the opening, a divider was placed in the center of the opening (in the range of 900 to 1500 [mm] from the bottom of the opening; see *Figure 3*).

A fire source was placed near the corner away from the opening to avoid influence from air ventilation. One SP system nozzle was placed on the center of the ceiling. The water pressure was 0.1 [MPa], and the corresponding water flow rate was 80 [l/min]. The sprinkler nozzle is made by “Senju sprinkler (product ZQR II), the performance number is K80, and nozzle diameter is $\phi 35$.

4.2 *Measurement parameters*

(1) Temperature

Measured temperatures were perpendicular distributions in the compartment and at the opening and outside air as shown in *Figure 2*. There were three thermocouples trees. The one in the left side corner was termed Tree A, that in the center Tree B, and that in the right side corner Tree C.

(2) Differential pressure

As shown in *Figure 3*, differential pressure at the opening was measured at three points in the vertical direction with a 300 [mm] interval below the opening and a 200 [mm] interval above the opening.

(3) CO_2 concentration

As shown in *Figures 2 and 3*, CO_2 concentration in the compartment was measured at two corners and the height was 0 and 2000 mm from the floor. It was also measured at the opening at the height of 2000 [mm] from the floor.

(4) Mass loss rate

Mass loss rate was measured with three load cells.

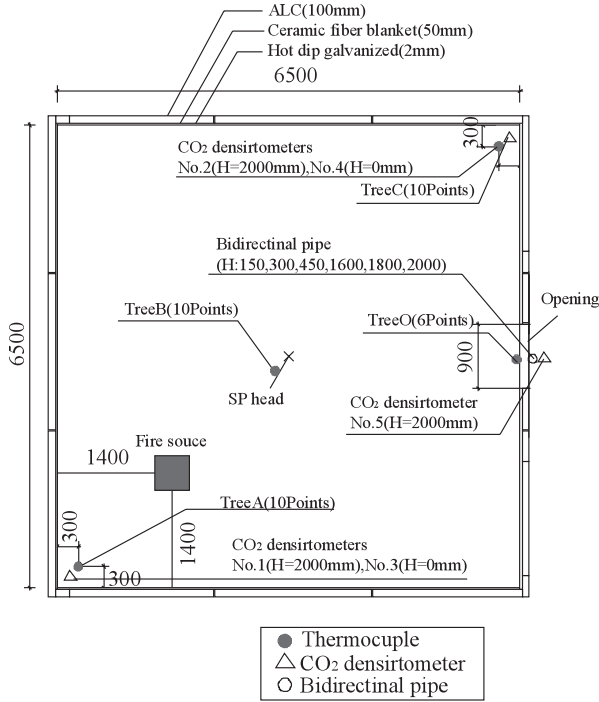


Figure 2 Floor plan of the experimental compartment [unit: mm]

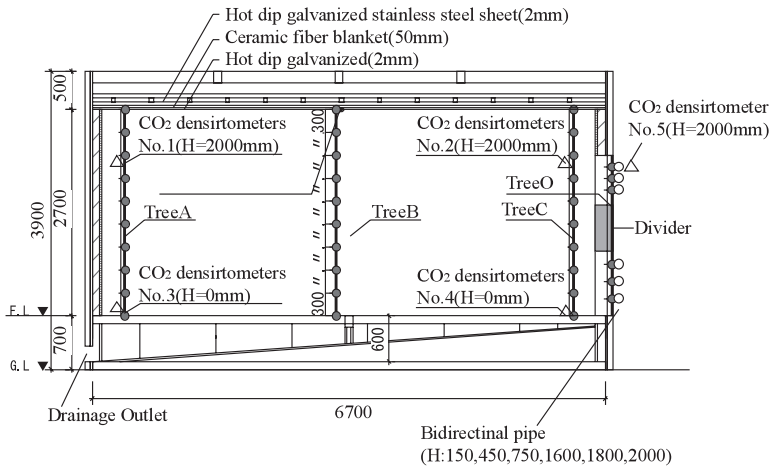


Figure 3 Cross-section of the experimental compartment [unit: mm]

4.3 Experimental condition

There were 12 combinations in this experiment by different fire sources and water flow rates. Table 1 is the list of the experimental conditions.

Table 1 Experimental conditions

Expt. No.	Fire Source		Water flow rate
	Fire area	Fuel amount	
1	0.1 m ²	2ℓ	0 ℓ/min
2			20 ℓ/min
3			40 ℓ/min
4			60 ℓ/min
5	0.2 m ²	4ℓ	0 ℓ/min
6			20 ℓ/min
7			40 ℓ/min
8			60 ℓ/min
9	0.4 m ²	8ℓ	0 ℓ/min
10			20 ℓ/min
11			40 ℓ/min
12			60 ℓ/min

4.4 Fire source

Figure 4 shows the rectangular pans used as a fire source in this experiment. In order to change the size of fire, the fire source area was changed in three ways: 0.1, 0.2 and 0.4 [m²]. Then 2 [ℓ] of methanol was poured into each pan per 0.1 [m²].

4.5 Sprinkler Application Scenarios

The water discharge amount was changed in four ways: 60, 40, 20 and 0 [ℓ/min]. However, in order to change the amount of water discharge, the water pressure needs to be adjusted, but the change in pressure may also change the flow of water droplets from the SP head. For that reason, water intake boxes were installed, as shown in Figure 5, and Water outside boxes was changed the water flow rate, without changing water pressure.

Figure 6 shows the relation between the watering area and the water flow rate after the water intake boxes were installed. In this study, it was necessary to measure the burning rate of the fire source accurately. Therefore, the water intake boxes were positioned to prevent the fire source from receiving water (refer to Figures 5 and 6).

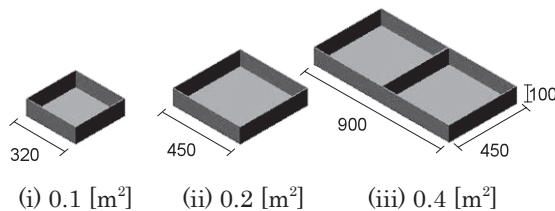


Figure 4 Rectangular fuel pans [mm]

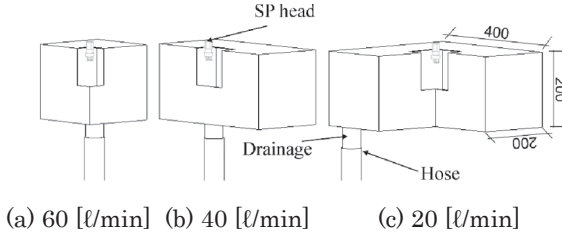


Figure 5 Water intake boxes [mm]

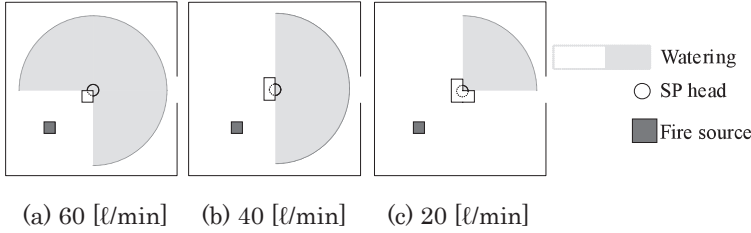


Figure 6 Conceptual diagrams for water distribution

5 EXPERIMENTAL RESULTS

5.1 Mass loss rate, Heat Release Rate, and CO₂ concentration

Table 2 shows the average mass loss rate of the fuel, and the volume fraction of CO₂ between 540 to 600 seconds when constant combustion was observed for each case. The table also shows the heat release rate, which is the result of mass loss rate multiplied by heat of combustion (22.4 [kJ/kg]) [8]. The mass loss rate was almost the same regardless of the amount of water applied as long as the size of the fire source was unchanged since this experiment used a design that intended to avoid watering the fire source directly.

The values of CO₂ concentration in the upper layer were stationary at all fire source sizes regardless of the amount of water applied. On the other hand, CO₂ concentration in the lower layer increased as the amount of water was increased, with a few exceptions.

Table 2 Average Mass loss rate and Volume fraction of CO₂ (in the range of 540 to 600 [sec.])

Condition		Mass Loss Rate [g/s]	Heat Release Rate [kW]	Volume fraction of CO ₂ [%]				
Fire Source	Water flow rate			Upper layer			Lower layer	
				No.1	No.2	No.5	No.3	No.4
0.1 m ²	0 l/min	2.3	53	0.67	0.61	0.57	0.04	0.05
	20 l/min	2.4	55	0.73	0.55	0.56	0.06	0.17
	40 l/min	2.5	57	0.58	0.56	0.51	0.05	0.11
	60 l/min	2.2	50	0.67	0.55	0.49	0.11	0.32
0.2 m ²	0 l/min	5.3	121	1.11	1.05	0.97	0.05	0.10
	20 l/min	5.1	117	1.07	0.89	0.91	0.05	0.09
	40 l/min	5.3	120	1.02	0.96	0.88	0.07	0.11
	60 l/min	5.2	117	1.21	1.07	0.95	0.10	0.33
0.4 m ²	0 l/min	11.3	255	1.64	1.63	1.48	0.04	0.08
	20 l/min	9.7	221	1.75	1.59	1.51	0.05	0.15
	40 l/min	10.9	246	1.66	1.63	1.57	0.06	0.09
	60 l/min	10.2	232	1.77	1.65	1.57	0.05	0.26

6 VALODATION OF GAS ANALYSIS (MOTHOD BASED ON THE COMPARISON OF FLOW RATES OPENING)

In order to verify the validity of the measurement method of the mass flow rate based on the gas analysis proposed in previous Section, a comparison of f mass flow rate was performed between the mass flow rates calculated from the flow rate distribution at the opening and the gas analysis. As for the gas concentration and the mass flow rate that were necessary for this verification, the post-ignition average rates between 540 to 600 [sec.] were used because the gas state in the compartment was in a quasi-steady state at this period.

6.1 Calculation from the flow rate distribution at opening

Figure 7 is a conceptual diagram presenting the flow distribution at the opening when the compartment was stratified into two layers. When the flow rate at the opening is $v(z)$ at the height of z , the outflow rate m can be expressed as follows:

$$m = \alpha \rho B \int v(z) dz \tag{23}$$

In this study, since it is difficult to measure the flow velocity at the opening in detail for each height, inflow rate was calculated by assuming that flow velocity are equal at a given height, as shown in Figure 8. Therefore, by using the flow velocity calculated from the differential pressure that was measured at each point, the outflow rate m_D was given by the following equation:

$$m_D = \alpha \rho_s B \sum h_1 v_n \tag{24}$$

Here, h_1 is 0.2 [m]. Similarly, the inflow rate at opening, m_a , was given by the following equation:

$$m_a = \alpha \rho_\infty B \sum h_2 v_n \tag{25}$$

Here, h_2 is 0.3 [m]. The coefficient for the opening, α , is 0.7 [-] for Equations 24 and 25 [9].

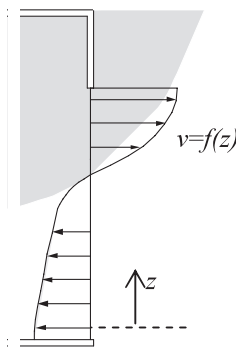


Figure 7 Conceptual diagram of flow velocity

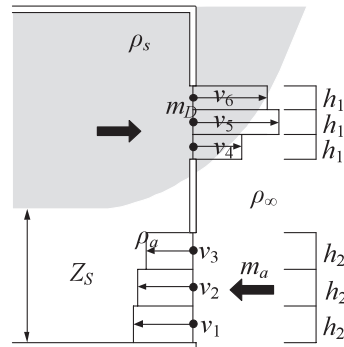


Figure 8 Conceptual diagram of flow rate

6.2 Calculation results

Figure 9 shows a comparison of the outflow rate m_D calculated by Equation 24 and the inflow rate m_a calculated from Equation 25. Figure 9 indicates that the value of m_D is greater than the one of m_a . The possible reason for this is air which came from gaps in the floor such as the drainage outlet.

6.3 Method based on the calculation with gas analysis

The following describes the calculation results of the outflow rate m_D based on the gas analysis (Equation 9). By substituting the average volume fraction of CO_2 (of Nos.1, 2, and 5 in Table 3) in Equation 19, the mass fraction of CO_2 , $Y_{CO_2}^S$, was calculated in order to calculate the outflow rate m_D . Also, the mass fraction of CO_2 in the outdoor air, $Y_{CO_2}^\infty$, was calculated by substituting the volume fraction of CO_2 in the atmosphere (0.03[%]) in Equation 20. For the burning rate m_f , the values in Table 2 were used.

Figure 10 is a comparison of the relation between the outflow rate m_D calculated from Equation 9 and the heat release rate of fire source Q_f . Figure 10 indicates that the outflow rate m_D increases as the heat release rate of the fire source increases. The possible reason for this is the increase in the ventilation rate due to the increased temperature of the upper layer along with the increase in the heat release rate.

On the other hand, the increase in the water flow rate does not significantly contribute to the change in the outflow rate at opening m_D . This is possibly attributed to the fact that the method used in this study avoided applying water into the fire source directly so that the heat release rate of the fire source was almost consistent regardless of the amount of the water applied.

6.4 Comparison of calculation results between gas analysis and the flow rate of opening

Figure 11 is a comparison of the flow rate at the opening based on gas analysis (Equations 9 and 10) and the flow velocity. Figure 11 indicates that the flow rate based on the gas analysis corresponds with the flow rate based on the flow velocity. As a note, it is reasonable to say that the measurement method based on the gas analysis is more reliable because it is not influenced by gaps while the method based on the flow velocity at the opening.

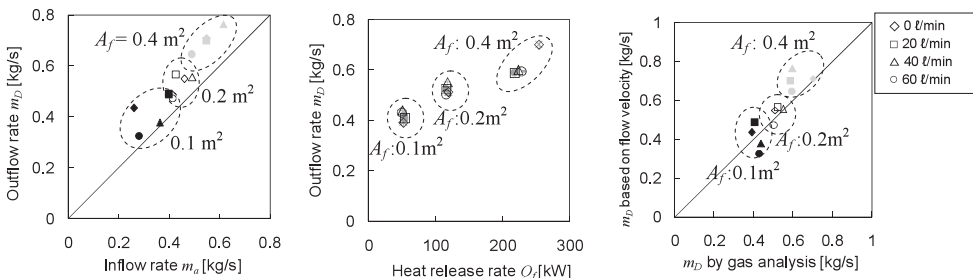


Figure 9 Flow rate of opening Figure 10 Outflow rate and HRR Figure 11 Comparison of outflow rate

7 VALODATION OF GAS ANALYSIS (COMPARISON WITH MASS LOSS RATE OF FUEL)

In order to verify the validity of the gas analysis method proposed in previous section, a comparison between the burning rate of fuel (methanol) based on the yield rate of CO_2 and the mass loss rate of fuel measured with load cells was performed by calculating the yield speed of CO_2 in the compartment, which is based on the CO_2 concentration and the flow rate where the airflow is coming in/out of the opening.

7.1 Estimation method for mass loss rate of fuel based on the gas analysis

When using methanol as a fuel, the burning rate m_f can be expressed by using the yield rate of CO_2 , Δm_{CO_2} , molecular weight of methanol (32), and CO_2 (44):

$$m_f = \frac{32}{44} \Delta m_{CO_2} \tag{26}$$

Next, since the concentration of O_2 in the compartment does not change if the compartment is in a steady state, the following equation can be formed for the yield rate of CO_2 , Δm_{CO_2} , outflow rate of CO_2 from the compartment, $Y_{CO_2}^s m_D$, and inflow rate of CO_2 to the compartment, $Y_{CO_2}^\infty m_a$:

$$\Delta m_{CO_2} = Y_{CO_2}^s m_D - Y_{CO_2}^\infty m_a \tag{27}$$

Here, m_D is the outflow rate at the opening, m_a is the inflow rate at opening, $Y_{CO_2}^s$ is the mass fraction of CO_2 in the upper layer, and $Y_{CO_2}^a$ is the mass fraction in the lower layer. Therefore, the burning rate m_f is given as follows:

$$m_f = \frac{32}{44} m_D (Y_{CO_2}^s - Y_{CO_2}^\infty) / \left(1 - \frac{32}{44} Y_{CO_2}^\infty \right) \tag{28}$$

7.2 Comparison between the estimated values of gas analysis and the measurement value by load cell

Figure 12 shows a comparison between the burning rate calculated from Equation 28 and the mass loss rate obtained by the load cell. In order to calculate the burning rate by Equation 28, it is necessary to acquire the outflow rate at opening m_D . The values obtained from the flow velocity distribution at the opening (Figure 9) were used.

Figure 12 indicates that the burning rate calculated from Equation 28 is fairly consistent with the mass loss rate by the load cell. As can be seen from Equation 28, this result indicates that it is possible to calculate the outflow rate m_D accurately from the burning rate of fuel m_f , and the CO_2 concentration of outside air or the upper layer.

8 DISCUSSION ON EACH MASS FLOW RATES

In order to predict the smoke behavior in a fire compartment with SP systems activation, it is necessary to grasp quantitatively the mass flow rate of fire plume, m_p , and downward airflow, m_E .

In this section, the comparison on the relation between the mass flow rates of fire plume, the downward airflow, the water flow rate, and the heat release rate, which were obtained by full scale experiment, are shown. In addition, the simple equations modelled on m_p and m_E are proposed and discussed.

8.1 Mass flow rate of fire plume

Figure 13 shows the relation between the flow rate of fire plume m_p calculated by Equation 12 and the water flow rate. As shown in Figure 13, it is noticeable that the mass flow rate of the fire plume increased as the water flow rate increased when fire source areas were 0.1 and 0.2 [m²]. The reason for this is possibly attributed to the disturbance in the air current of the lower layer due to the increase of water flow rate, and this may have caused the entrainment air flow to increase. On the other hand, when the fire source area was 0.4 [m²], the mass flow rate of the fire plume m_p was generally consistent regardless of the change in water flow rate. It is presumed that the buoyant velocity of the fire plume is greater if the fire source area (heat release rate) is greater such that the influence of the air flow disturbance caused by watering becomes comparatively less.

Figure 14 indicates the relation between the mass flow rate of the fire plume m_p and the heat release rate Q_f . The straight line in Figure 14 is the calculated result of the regressions for each water flow rate by assuming that the mass flow rate of the fire plume m_p can be expressed as an exponentiation of the heat release rate Q_f . As shown in Figure 14, the slopes of the regressions were 0.062 at 60 [l/min], 0.16 at 40 [l/min], 0.22 at 20 [l/min] and 0.38 at 0 [l/min]. This indicates that the dependency of the mass flow rate of the fire plume m_p to the heat release rate Q_f becomes less as the water flow rate becomes greater. Generally, the mass flow rate of the fire plume also varies depending on the entrained height (the height from the surface of the fire source to the boundary surface of the smoke layer). It is necessary to investigate the relation between the mass flow rate of the fire plume and the water flow rate further with respect to entrained height.

The mass flow rate of the fire plume in the persistent flame region under a calm condition is proposed by Zukoski as follows.

$$m_p = 0.447 \rho_a D Z^{3/4} \quad (29)$$

The mass flow rate of the fire plume in the persistent flame region under a calm condition is proposed by Heskestad as follows.

$$m_p = 0.0054 Q_c Z / \left(0.166 Q_c^{2/5} + Z_0' \right) \quad (30)$$

$$Z_1 = Z_0' + 0.166 Q_c^{2/5}$$

Where, Q_c is the heat Release Rate [kW/m^2], Z is the flame heights [m], Z_0' is the basic heights which the rate of heat release of flame ejected [m], and Z_l is the height of the average flame [m]. Where, ρ_a is the density of lower layer [kg/m^3], D is the diameter of the flame [m], and Z is the flame heights [m]. Although these formula means being proportional to each $\rho_a DZ$ or $Q_c Z/Z_l$, these is tried to confirm how much the volume of the fire plume is affected in the condition of the inside of the compartment disturbed by the high-pressured water droplets of SP systems such as this experiment.

Figure 15 indicates the relation between the mass flow rate of the fire plume in the persistent flame region m_p and " $\rho_a DZ$ ". As shown in Figure 15, the mass flow rate of the fire plume in the persistent flame region indicates about 2.4 times of the Equation 29 at fire Source $0.4[\text{m}^2]$. and about 2.8 times of ones at fire Source $0.1[\text{m}^2]$ regardless of the watering rates. The mass flow rate of the fire plume increased it more at the Small heat Release Rate than the large heat Release.

Figure 16 indicates the relation between the mass flow rate of the fire plume in the persistent flame region m_p for the mass flow rate, and the flame heights Z for the height of the average flame Z_l . As shown in Figure 16, the mass flow rate of the fire plume in the persistent flame region indicates about 1.3 times of the Equation 30 to 2.2 times.

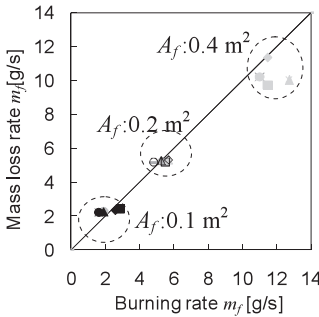


Figure 12 Mass loss rate and Burning rate

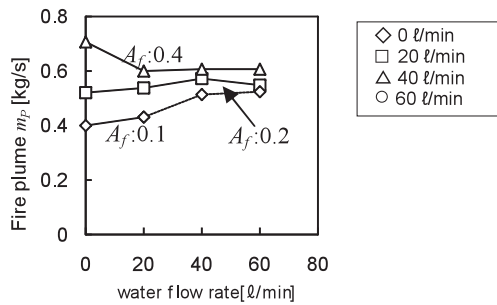


Figure 13 Comparison between water flow rate and m_p

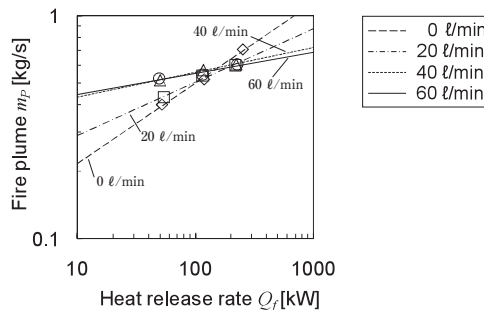


Figure 14 Comparison between HRR and m_p

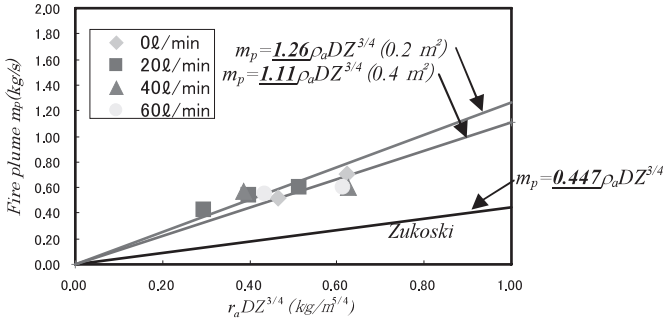


Figure 15 Mass flow rate of the fire plume, m_p (Zukoski)

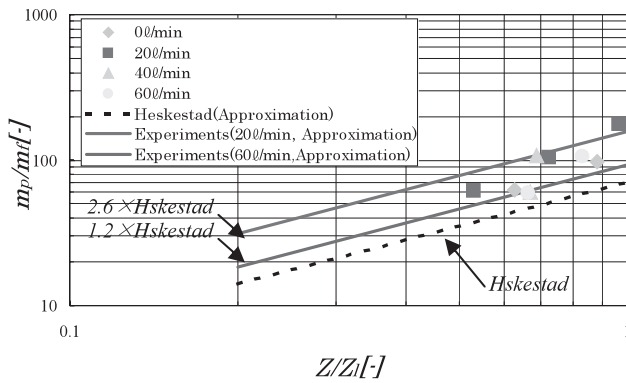


Figure 16 Mass flow rate of the fire plume, m_p (Heskestad)

8.2 Mass flow rate of downward airflow

Figure 17 shows the relation between the mass flow rate of downward airflow calculated from Equation 11 and the water flow rate for each fire source area. The mass flow rate of downward airflow also increases as the water flow rate increases, with a few exceptions. Also, as the fire source area (the heat release rate) increases, the mass flow rate of downward airflow m_E decreases comparatively. Thus, it is presumed that the mass flow rate of downward airflow m_E may have a great influence on the temperature (buoyancy) of the upper layer. Further investigation of the relation between the temperature of the upper layer and the flow rate of downward airflow is needed.

A relationship between the ratio of the mass flow rate penetrated to lower layer by water droplets to the mass flow rate of watering supply from SP, and the ratio of the upper (smoke) layer and the lower layer obtained from the experiment is shown in Figure 18. As a result, the following equation is obtained by regression analysis.

$$m_E = \frac{0.003}{(\rho_a - \rho_s) / \rho_s} m_{SP} \tag{31}$$

Although the experimental condition is not enough, when the mass flow rate of watering supply from SP, m_{sp} , and temperature at the smoke and lower layers are known, the mass flow rate penetrated to lower layer can be computed by Equation 31.

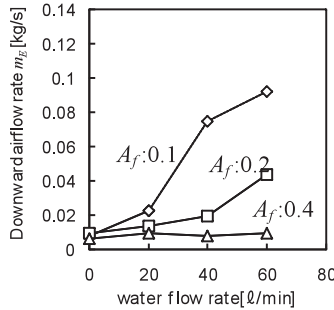


Figure 17 Comparison between downward airflow and water flow rate

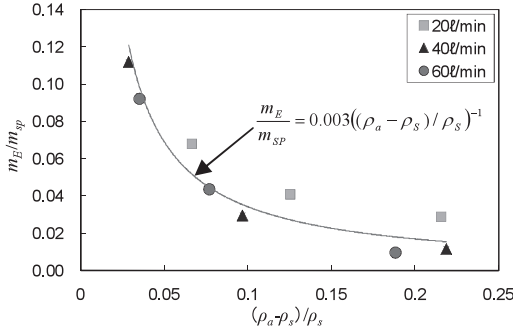


Figure 18 Comparison between the mass flow rate and the density

9 CONCLUSION

The ultimate goal of this study was to develop a predictive model for smoke behavior during SP system activation, and as a first step, this combustion experiment was conducted using a full-scale fire compartment. As a result, the following aspects were confirmed.

- By performing gas analysis on the upper and the lower layers, a measurement method of flow rates for the fire plume, the downward airflow, and in/outflow at the opening was introduced, and was confirmed as a method that provides adequate measurement accuracy.
- The disturbance in air flow caused by watering influences the fire plume and the entraining rate increases. Also, the rate of increase in the flow rate of the fire plume with respect to the increase of the heat generation rate becomes comparatively smaller as the water flow rate increases.

- Downward airflow is generated by the droplets of water from the pressurized discharge during SP system activation. Also, the mass flow rate of downward airflow m_E increases as the water flow rate increases and the heat release rate of the fire source decreases.
- Although the experimental condition is not enough, when the mass flow rate of watering supply from SP, m_{SP} , and the densities of the upper and lower layers are known, the mass flow rate penetrated to lower layer, m_E , can be computed by Equation 30.

ACKNOWLEDGMENTS

The authors would like to thank Mr. F. Takase and Mr. T. Orito (Graduate students, Tokyo University of Science) for support of this experiment.

REFERENCES

1. MLIT Building Guidance Division, Building Center of Japan, et al. Ed., Guide and Computation for the Evacuation Safety Verification Method 2001, 2001 (in Japanese)
2. Y. L. Cooper, The interaction of an isolated sprinkler spray and a two-layer compartment fire environment: Phenomena and model simulations, *Fire Safety Journal*, Vol.25, 89-107, 1995
3. E. E. Zukoski, T. Kubota, and B. Cetegen, Entrainment in Fire Plumes, *Fire Safety J.*, Vol.3, No.2-4, 1981
4. B. M. Cetegen, E. E. Zukoski, and T. Kubota, Entrainment in the Near and Far Field of Fire Plume, *Combustion Science and Technology*, Vol.39, 305-331, 1984
5. J. Prahl and H. W. Emmons, Fire induced flow through an opening, combustion and flame, *Journal of Fire Protection Engineering*, Vol.25(3), 369-385, 1975
6. I. Nakaya, T. Tanaka, and M. Yoshida, Doorway flow induced by a propane fire, *Fire Safety Journal*, Vol.10, 185-195, 1986
7. J. Yamaguchi, S. Yamada, T. Tanaka, and T. Wakamatsu, Measurement for Mass Flow Rate of Door Jet in Compartment Fires, *Journal of Architecture, Planning and Environmental Engineering*, Transactions of AIJ, No.501, 1-7, 1997 (in Japanese)
8. SFPE Handbook of Fire Protection Engineering 3rd ed., Appendix C Table C.2, 2002
9. T. Tanaka, Introduction to Fire Safety Engineering for Building Design, Building Center of Japan, 14, 2001 (in Japanese)